A J^{CH}-Modulated 2D (HACACO)NH Pulse Scheme for Quantitative Measurement of $^{13}C^{\alpha}$–$^{1}H^{\alpha}$ Couplings in ^{15}N, ^{13}C-Labeled Proteins[1]

T. Kevin Hitchens,* Scott A. McCallum,† and Gordon S. Rule*,†,[2]

*Department of Biological Sciences, Carnegie Mellon University, 4400 Fifth Avenue, Pittsburgh, Pennsylvania 15213; and
†Department of Biochemistry, University of Virginia School of Medicine, Charlottesville, Virginia 22908

A triple-resonance pulse sequence is presented for the quantitative measurement of $^{1}H^{\alpha}$–$^{13}C^{\alpha}$ single-bond couplings in ^{15}N, ^{13}C uniformly labeled proteins. This $^{1}J^{CH}$-modulated (HACACO)NH experiment yields $^{1}H_N$–^{15}N-correlated 2D spectra in which the amplitude of each peak is modulated by the $^{1}H^{\alpha}$–$^{13}C^{\alpha}$ J coupling of the preceding residue, $(i - 1)$. The experiment is demonstrated on a 1.0 mM sample of Rho130, the 15-kDa RNA binding domain of *E. coli* Rho factor. The average error in the measured coupling constants was less than 0.8%. This sequence allows the measurement of the $^{1}J^{CH}$ couplings from a proton–nitrogen HSQC without the need for assigning the H^{α} and C^{α} resonances. © 1999 Academic Press

Key Words: C–H residual dipole coupling; pulse sequence; (HACACO)NH.

Residual single-bond dipolar couplings are highly effective restraints for improving structures determined by NMR methods (*1*). The single-bond dipolar coupling provides direct information as to the orientation of the bond vector with respect to the anisotropic alignment tensor of the molecule. Thus, these couplings provide global structural information rather than the local information traditionally derived from distance and torsional angle constraints. The dipolar couplings are generally measured from samples in which the protein is slightly oriented by co-solute particles, such as lipid bicells (*2*) or filamentous bacteriophage particles (*3*). The single-bond dipolar coupling in these samples manifests itself as a change in the corresponding ^{1}J splitting relative to the splitting due to the scalar interaction alone. Therefore, the development of convenient and accurate methods for determining J splittings is necessary to fully utilize residual dipolar coupling in structure refinement.

There are two basic methods for measuring single-bond J splittings. The first method directly measures the separation of doublets in coupled spectra. For example, ^{1}H–^{15}N coupling can be determined by collecting an HSQC spectrum without heteronuclear decoupling in either the ^{1}H or the ^{15}N dimension (*4*). This method is useful for well-resolved spectra from small proteins. However, due to the doubling of resonance lines it becomes increasingly more difficult to resolve peaks as the protein size increases. This problem is particularly acute for the measurement of ^{1}H–$^{13}C^{\alpha}$ couplings due to the poor chemical shift dispersion in this region of the ^{1}H–^{13}C-correlated spectrum. This problem can be somewhat alleviated by collecting two different ^{1}H–^{13}C HSQC spectra in which each individual resonance peak in a coupled pair is collected separately (*5*). Alternatively, the resonances can be resolved by evolving a third indirectly detected dimension such as in the (HA)CA-(CO)NH experiment reported by Tjandra and Bax (*6*). Recently, Kay and co-workers reported a 3D HNCO-based pulse scheme for measuring $^{1}H^{\alpha}$–$^{13}C^{\alpha}$ couplings (*7*). This sequence has the dual advantage of decreasing resonance overlap by the additional third dimension as well as collecting each component of the doublet in two separate 3D spectra. However, underdigitization in the indirectly detected dimensions and unresolved $^{13}C^{\beta}$–$^{13}C^{\alpha}$ couplings would be expected to lead to a reduction in the accuracy of the measurement of smaller couplings in moderately sized proteins (10–20 kDa).

The second method for measuring J splittings is based on intensity modulation of a resonance peak. This method has been applied to the measurement of both $^{1}H_N$–^{15}N and ^{1}H–^{13}C couplings (*8, 9*). The advantages of this approach over direct measurement of the coupling constant are a reduction in the complexity of the spectra and a more straightforward analysis of the experimental error of the coupling. Generally the $^{1}H_N$–^{15}N-correlated spectrum is sufficiently well resolved in moderately sized proteins such that it is possible to determine the coupling for the majority of the residues directly from the spectrum. However, the corresponding ^{1}H–^{13}C-correlated spectrum is usually poorly resolved in the alpha region, limiting the number of residues for which the coupling can be measured. Although this limitation could be overcome by the addition of a third frequency dimension, the additional time required for digitization of this dimension severely limits the number of intensity-modulated spectra that could be obtained. Conse-
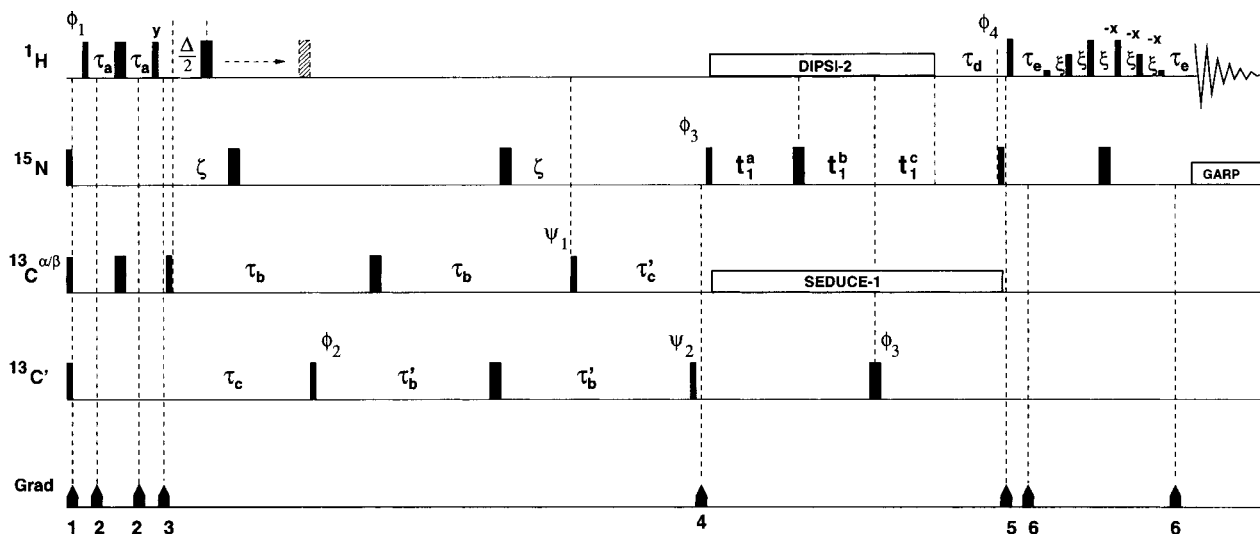
FIG. 1. Pulse scheme for the $^1J^{CH}$-modulated (HACACO)NH experiment. Narrow and wide rectangular blocks represent RF pulses of 90° and 180° flip angles, respectively. Proton pulses were applied at the solvent frequency. The DIPSI-2 decoupling scheme (*17*) was applied with a field strength of 4 kHz. The nitrogen carrier frequency was set to 116 ppm, and the GARP decoupling scheme (*18*) was applied at a field strength of 1.2 kHz. The carrier frequency for $C^{\alpha/\beta}$ and C′ channels were set at 42.5 and 175 ppm, respectively and pulses were applied at a field strength such that the excitation of the other carbon spin was minimal. The delays used were $\tau_a = 1.6$ ms, $\tau_b = \tau_b' = 14$ ms, $\tau_c = \tau_c' = 9$ ms, $\tau_d = 5.5$ ms, $\tau_e = 2.7$ ms, $\zeta = \tau_b - \tau_c$ (5 ms), and $\xi = 210$ μs. Carbonyl decoupling was accomplished utilizing a SEDUCE-1 scheme (*19*) at a field strength of 1.25 kHz. Pulsed field gradients are employed at various points during the sequence for *zz*-magnetization filters and π-clean filters. Rectangular gradient pulses were applied at times and power levels as follows: G_z1 (0.9 ms, 8 G/cm), G_z2 (0.5 ms, 4 G/cm), G_z3 (0.5 ms, 16 G/cm), G_z4 (0.5 ms, 10 G/cm), G_z5 (0.5 ms, 20 G/cm), and $G_x6 = G_y6 = G_z6$ (0.7 ms, 10 G/cm). Phase cycling was $\phi_1 = x, -x$; $\phi_2 = 2(x), 2(-x)$; $\phi_3 = 4(x), 4(-x)$; $\phi_4 = -x$; and $\phi_{REC} = x, -x, -x, x, -x, x, x, -x$. Phase corrections were applied ($\psi_1 = \psi_2 = 30°$) to compensate for the phase changes induced by Bloch–Siegert shifts. The States method of quadrature detection was used by incrementing the phase of ϕ_3 by 90° (*20*). Water suppression was achieved by a WATERGATE-type sequence (*21*) of six proton pulses with equivalent power and pulse widths equal to 0.231, 0.692, 1.462, 1.462, 0.692, and 0.231 of the proton 90° pulse width, respectively, during the last coherence transfer period.

quently, it would be more useful if the intensity modulation of the signal due to ^1H–^{13}C coupling could be relayed to the more resolved ^1H_N–^{15}N 2D spectrum. In this Communication, we present a pulse scheme for measuring $^1H^\alpha$–$^{13}C^\alpha$ couplings from a series of intensity-modulated 2D ^1H_N–^{15}N-correlated spectra.

Figure 1 illustrates the (HACACO)NH pulse scheme for the quantitative measurement of single-bond $^1H^\alpha$–$^{13}C^\alpha$ J^{CH} couplings with ^{15}N- and ^{13}C-labeled proteins. The magnetization transfer pathway in this two-dimensional $^1J^{CH}$-modulated experiment is similar to other 3D frequency correlation HA(CACO)NH experiments (*10, 11*); therefore, only a brief description of the coherence pathway is presented here. The major differences for this new pulse sequence are additional overlapping of coherence transfer steps (*12*), refocusing of C^α–C^β coupling, and semi-constant time evolution of the ^{15}N chemical shift (*13*).

The initial INEPT sequence transfers the initial $^1H^\alpha$ magnetization to antiphase ^1H–$^{13}C^\alpha$ coherence. The density matrix then simultaneously evolves under the influence of scalar coupling to each of the four bound spins: H^α ($J^{C\alpha H\alpha}$), ^{15}N ($J^{C\alpha N}$), $^{13}C^\beta$ ($J^{C\alpha C\beta}$), and the carbonyl, C′ ($J^{C\alpha C'}$). A key feature of this pulse sequence is that the antiphase $^{13}C^\alpha$–H^α magnetization refocuses to in-phase $^{13}C^\alpha$ magnetization for the variable delay, Δ. This variable delay results in the final signal being amplitude modulated by a factor of $\sin(\pi J^{CH}\Delta)$. Since the $^{13}C^\alpha$–^{15}N

coupling evolves for the period ζ–$(\tau_b-\zeta)$ + $(\tau_b-\zeta)$–ζ, and the $^{13}C^\alpha$–$^{13}C^\beta$ coupling is refocused at the end of the τ_b–$\pi(C^{\alpha/\beta})$–τ_b period ($\tau_b = \frac{1}{2J}^{C\alpha C\beta}$) there is no net evolution of the $^{13}C^\alpha$ magnetization due to coupling to either $^{13}C^\beta$- or ^{15}N-bound spins. For the case of glycine, the absence of $^{13}C^\alpha$–$^{13}C^\beta$ coupling causes the relevant signal to be inverted relative to the signal from other residues. During the period τ_c ($\frac{1}{2J}^{C\alpha C'}$), the $^{13}C^\alpha$ magnetization becomes antiphase with respect to $^{13}C'$, and the subsequent $\pi/2$ ($^{13}C'$) pulse generates double-quantum $^{13}C^\alpha$–$^{13}C'$ magnetization which does not evolve further under $J^{C\alpha C'}$ coupling. Subsequent coherence transfer steps are similar to the published 3D HA(CACO)NH experiments (*10, 11*) with the exception that the ^{15}N frequency labeling is achieved in a "semi-constant time" manner to allow for increased digitization in this dimension.

A series of (HACACO)NH experiments acquired with different $^{13}C^\alpha$–$^1H^\alpha$ refocusing delays, Δ, yields ^1H_N–^{15}N-correlated 2D spectra in which each amide resonance peak (*i*) is amplitude modulated by the apparent $^1J^{CH}$ coupling for the $^{13}C^\alpha$–$^1H^\alpha$ spins of the preceding ($i - 1$) residue. For oriented protein samples, the apparent coupling would be equal to the sum of the scalar single-bond coupling and the residual dipolar coupling. For resonance peaks corresponding to residues that are preceded by a glycine, the frequency modulation is equal to the sum of the two methylene $^{13}C^\alpha$–$^1H^\alpha$ couplings (*14*). Al-
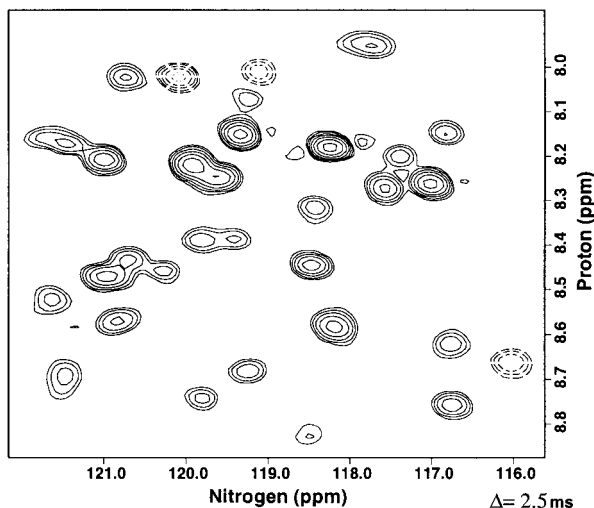
FIG. 2. A section of the NMR spectrum from the (HACACO)NH experiment with a 1.0 mM sample of ^{15}N, ^{13}C uniformly labeled Rho130. The data shown were collected with a delay $\Delta = 2.5$ ms; all increments of Δ were collected with 64 transients per t_1 increment and dimensions of $104(t_1) \times 512(t_2)$ complex points. The sweep width in ω_1 was 2 kHz. The data were processed to a 3D matrix $16(\Delta) \times 512(t_1) \times 512(t_2)$ using a shifted sine-squared apodization in both frequency dimensions (75° shift for nitrogen and 65° shift for proton). The broken contour levels indicate negative peaks.

though the individual residual dipolar couplings cannot be resolved for these methylene sites, their sum may be used directly in structure calculations and this restraint is similar in information content to that obtained from single $^{13}C^{\alpha}-^{1}H^{\alpha}$ residual dipolar couplings (*14*).

Since the $^{1}J^{CH}$ modulation in the $^{1}J^{CH}$ (HACACO)NH experiment occurs in a "constant time" fashion, with simultaneous coherence transfer and magnetization refocusing times, the only signal decay that can occur is due to differences between the relaxation rates of the in-phase and antiphase $^{13}C^{\alpha}$ transverse magnetization. In practice, this difference is negligible and can be ignored. Thus, the signal intensity is fit with

$$I(\Delta) = A \sin(\pi J^{CH}\Delta), \qquad [1]$$

where $I(\Delta)$ is the peak intensity for a $^{1}J^{CH}$-modulation delay of Δ, and the constant A is the peak intensity for $\Delta = \frac{1}{2J}$ (A is negative for residues preceded by Gly). When fitting the data, a time equal to $\pi/2$ times the carbon 90° pulse length must be added to Δ.

Measurement of $^{1}J_{CH}$ is demonstrated on a 1.0 mM sample of uniformly ^{15}N/^{13}C-labeled 15-kDa RNA binding domain of *E. coli* Rho factor, Rho130 (*15*). The NMR sample was prepared in water containing 5% D$_2$O, 10 mM potassium phosphate buffer, pH 7, and 150 mM K$_2$SO$_4$. The NMR spectra were recorded at 25°C on a Bruker DRX-600 spectrometer, equipped with a 5 mM triple-resonance, triple-axis gradient probe. The data were collected as a pseudo 3D experiment with a total of 16 of different Δ times. The initial delay of $\Delta = 0.5$

ms was followed by 15 subsequent increments of 1 ms. The data were transformed into a 3D matrix with Felix 97 (Molecular Simulations Inc., San Diego, CA). The peak intensities were obtained by taking an orthogonal vector through the matrix at the maximum of each peak.

Figure 2 shows a section of the J^{CH}-modulated (HACACO)NH spectrum for Rho130 at a delay (Δ) of 2.5 ms. Note that the negative resonance peaks correspond to magnetization that originates from $(i - 1)$ glycine residues. Since the peak intensity is sine modulated, an intensity of zero was included in the data at $\Delta = 0$. The 17 data points were fit to Eq. [1] with the nonlinear least-squares fitting software NONLIN (*16*). Figure 3 shows representative intensity data for a nonglycine and
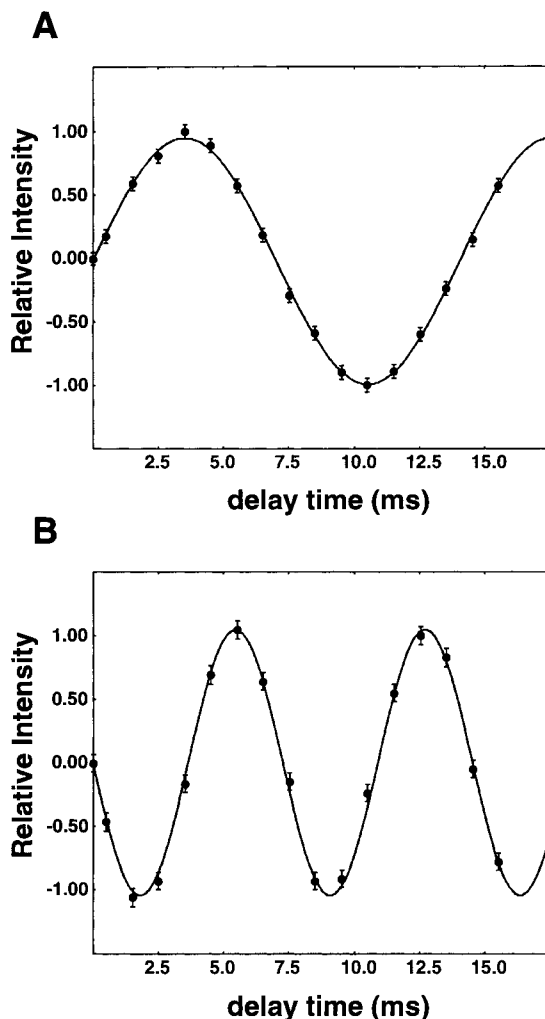

FIG. 3. Representative J^{CH}-modulated curves obtained with the (HACACO)NH experiment for residues Asp52 (A) and Gly63 (B). Intensity points for all data were extracted with a Felix 97 macro that extracts the peak intensities of the orthogonal vector through the maximum intensity of each peak ($\Delta \sim \frac{1}{2J}^{CH}$). Error bars represent peak-to-peak signal to noise for the peak maximum, and the curve represents the least-squares best fit determined by NONLIN with a 67% confidence interval: Asp52, $^{1}J^{CH} = 142.2$ (141.7 143.1) Hz; and Gly63 ($^{1}J^{CH1} + ^{1}J^{CH2}$) $= 275.4$ (274.2 276.5) Hz.

a glycine residue in Rho130. Of the observable 123 amide resonances it was possible to determine $^1J^{CH}$ values for 81 nonglycine residues and $^1J^{CH1} + {}^1J^{CH2}$ values for 10 glycine residues, with an average error in the J value of less than 0.8%.

In conclusion, the J^{CH}-modulated (HACACO)NH sequence provides a means for utilizing the well-characterized H_N–^{15}N-correlated spectrum to measure the coupling between H^α and C^α spins. Of course, this implies that it is not necessary to have knowledge of the H^α/C^α assignments prior to the utilization of the orientation of the H^α–C^α bond vector in the structural refinement. This feature of the experiment may be particularly useful for detecting ligand-induced structural and dynamic changes in proteins without the need for reassigning more than the amide chemical shifts for the ligand-bound protein.

We have demonstrated the utility of this pulse scheme on a 15-kDa $^{13}C/^{15}N$-labeled protein. The overlapping coherence transfer steps employed in the sequence result in efficient transfer of magnetization that will aid in the application to larger protein systems. We anticipate that this sequence will be applicable to fully protonated proteins up to a molecular weight of approximately 20–25 kDa based upon expected relaxation rates (22). Additionally, a small gain in sensitivity may be achieved by employing a $^1H^\alpha$ selectively labeled, ^2H-, ^{13}C-, ^{15}N-labeling scheme (22).

ACKNOWLEDGMENTS

REFERENCES

1. N. Tjandra, J. G. Omischinski, A. M. Gronenborn, G. M. Clore, and A. Bax, Use of dipolar ^1H–^{15}N and ^1H–^{13}C couplings in the structure determination of magnetically oriented macromolecules in solution, *Nature Struct. Biol.* **4**, 732–738 (1997).

2. N. Tjandra and A. Bax, Direct measurements of distances and angles in biomolecules by NMR in dilute liquid crystalline media, *Science* **278**, 1111–1114 (1997).

3. M. R. Hansen, L. Meuller, and A. Pardi, Tunable alignment of macromolecules by filamentous phage yields dipolar coupling interactions, *Nature Struct. Biol.* **5**, 1065–1074 (1998).

4. A. Bax and N. Tjandra, High-resolution heteronuclear NMR of human ubiquitin in an aqueous liquid crystalline medium, *J. Biomol. NMR* **10**, 289–292 (1997).

5. M Ottiger, F. Delaglio, and A. Bax, Measurement of J and dipolar couplings from simplified two dimensional NMR spectra, *J. Magn. Reson.* **131**, 373–378 (1998).

6. N. Tjandra and A. Bax, Large variations in $^{13}C^\alpha$ chemical shift anisotropy in proteins correlate with secondary structure, *J. Am. Chem. Soc.* **119**, 9576–9577 (1997).

7. D. Yang, J. Tolman, N. K. Goto, and L. E. Kay, An HNCO-based pulse scheme for the measurement of $^{13}C_\alpha$–$^1H_\alpha$ one-bond dipolar couplings in ^{15}N–^{13}C labeled proteins, *J. Biomol. NMR* **12**, 325–332 (1998).

8. N. Tjandra, S. Grzesiek, and A. Bax, Magnetic field dependence of nitrogen–proton J splittings in ^{15}N-enriched ubiquitin resulting from relaxation interference and residual dipolar coupling, *J. Am. Chem. Soc.* **118**, 6264–6272 (1996).

9. N. Tjandra and A. Bax, Measurement of dipolar contributions to $^1J_{CH}$ splittings from magnetic-field dependence of J modulation in two-dimensional NMR spectra, *J. Magn. Reson.* **124**, 512–515 (1997).

10. R. Jerala and G. S. Rule, A sensitive triple-resonance pulse sequence to elucidate correlations between H^i_α, N^{i+1}, and H_N^{i+1} nuclei, *J. Magn. Reson. B* **110**, 87–90 (1996).

11. W. Feng, C. B. Rios, and G. T. Montelione, Phase labeling of C–H and C–C spin-system topologies: Application in PFG-HACANH and PFG-HACA(CO)NH triple-resonance experiments for determining backbone resonance assignments in proteins, *J. Biomol. NMR* **8**, 98–104 (1996).

12. C. Bracken, A. G. Palmer, and J. Cavanagh, (H)N(COCA)NH and NH(COCAH)NH experiments for ^1H–^{15}N backbone assignments in $^{13}C/^{15}N$-labeled proteins, *J. Biomol. NMR* **9**, 94–100 (1997).

13. S. Grzesiek and A. Bax, Amino acid type determination in the sequential assignment procedure of uniformly $^{13}C/^{15}N$-enriched proteins, *J. Biomol. NMR* **3**, 185–204 (1993).

14. M. Ottiger, F. Delaglio, J. Marquardt, N. Tjandra, and A. Bax, Measurement of dipolar couplings for methylene and methyl sites in weakly oriented macromolecules and their use in structure determination, *J. Magn. Reson.* **134**, 365–369 (1998).

15. D. M. Briercheck, T. C. Wood, T. J. Allison, J. P. Richardson, and G. S. Rule, The NMR structure of the RNA binding domain of *E. coli* rho factor suggests possible RNA–protein interactions, *Nature Struct. Biol.* **5**, 393–399 (1998).

16. M. L. Johnson and S. G. Frasier, Nonlinear least-squares analysis, *Methods Enzymol.* **117**, 301–342 (1985).

17. A. J. Shaka, C. J. Lee, and A. Pines, Iterative schemes for bilinear operators: Application to spin decouplings, *J. Magn. Reson.* **77**, 274–293 (1988).

18. A. J. Shaka, P. B. Barker, and R. Freeman, Computer optimized decoupling scheme for wide band applications and low-level operation, *J. Magn. Reson.* **64**, 547–552 (1985).

19. M. McCoy and L. Mueller, Selective shaped pulse decoupling in NMR: Homonuclear [^{13}C] carbonyl decoupling, *J. Am Chem. Soc.* **114**, 2108–2112 (1992).

20. D. J. States, R. A. Haberkorn, and D. J. Ruben, A two-dimensional nuclear Overhauser experiment with pure absorption phase in four quadrants, *J. Magn. Reson.* **48**, 286–292 (1982).

21. V. Skelenar, M. Piotto, R. Leppik, and V. Saudek, Gradient-tailored water suppression for ^1H–^{15}N HSQC experiments optimized to retain full sensitivity, *J. Magn. Reson. A* **102**, 241–245 (1993).

22. T. Yamazaki, H. Tochio, J. Furui, S. Aimoto, and Y. Kyogoku, Assignment of backbone resonances for larger proteins using the ^{13}C–^1H coherence of a $^1H_\alpha$-, ^2H-, ^{13}C-, and ^{15}N-labeled sample, *J. Am. Chem. Soc.* **119**, 872–880 (1997).